Dummy Load Prototype Design for ITER Coil Power Supply System

C. Li, M. Zhang, K. X. Yu, X. Q. Qin, Z. Q. Song, and P. Fu

***Abstract*— This paper mainly introduces the design of the dummy load prototype, whose functions are to verify the capability of the International Thermonuclear Experimental Reactor magnetic power supply systems to operate at their rated power levels without energizing the superconducting coils. The rated inductance is 6.73 mH and the extreme pulse operation mode is 68 kA/15 s ON and 900 s OFF. Therefore, in order to meet the special requirements of the large inductance and the large pulse test current, a structure of dry-type air-core water-cooling prototype with epoxy resin casting technique is presented. The finite-element simulation analysis is introduced in detail, focusing on the thermal performance and dynamic stability, especially under the extreme pulse operation condition. In addition, the electromagnetic environment around the dummy load is also analyzed to provide the input for the instrumentations selection and the delimitation of personal safe area. Finally, seismic analysis is introduced to verify the antiseismic property of the dummy load.**

***Index Terms*— Dummy load, dynamic stability, finite element, seismic.**

I. Introduction

INTERNATIONAL Thermonuclear Experimental Reactor (ITER) is an international nuclear fusion project to realize an experimental fusion reactor based on the concept of a tokamak. The poloidal field (PF) converter module is an important component of the ITER equipment in the plasma shape and position control in the vertical and horizontal directions [1]–[3]. As an inductive component, the dummy load is mainly used to verify the capability of the power supply systems to operate at their rated power levels without energizing the superconducting coils (SC). For example, it can be used to test converters, switching networks, discharge circuits, and so on.

II. Converter Module and Requirments

The topology of the PF converter unit is shown in Fig. 1. The PF ac/dc converter unit consists of a rectifier transformer, converter module, bypass, dc reactors, disconnectors, etc. The converter module is composed of four converter bridges with one dc reactor connected in series, realizing the 4-quadrant operational mode [4]. The SC load is replaced by a dummy load when the components need to be tested without energizing the SC. According to the specified functions and operational modes, the requirements of the dummy load are listed as shown in Table I. The currents of 45, 55, and 68 kA are the representative values of central solenoid coils, PF coils, and toroidal field coils, respectively. The rated inductance is 6.73 mH with the precision ±1% and the rated direct current is 7.75 kA. Due to various testing requirements, the dummy load should operate under different modes. The most typical pulse mode is 68 kA lasting 15 s, and then operating with zero current for 900 s. Therefore, the structural performance and thermal stability are essential considerations for the design of the dummy load, which is proposed in this paper.

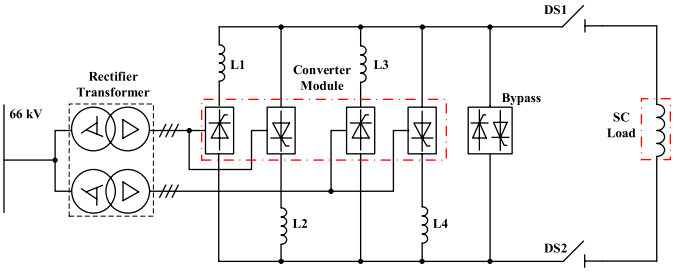

Fig. 1. Topology of PF converter module.

TABLE I
Main Requirements for Dummy Load

Parameters	Values
Rated inductance, mH	6.73±1%
Rated continuous current, kA	7.75
Operating ambient temperature, °C	-25~45
Pulse operational modes: current, duty cycle	45 kA, 30 s on/900 off; 55 kA, 20 s on/900 s off; 68 kA, 15 s on/900 s off
Insulation level, Nominal /testing /impact, kV	AC, 12/28/75; DC, 12
Cooling medium	Demineralised water
Shape, conductor material	Cylinder, Aluminum
Location	Outdoor

III. Prototype and Structure

Considering the rigorous requirements in the thermal and dynamic stability due to the various operational modes,

Manuscript received July 22, 2015; revised April 26, 2016; accepted June 23, 2016. Date of publication July 12, 2016; date of current version September 9, 2016.

C. Li, M. Zhang, and K. X. Yu are with the State Key Laboratory of Advanced Electromagnetic Engineering and Technology, Huazhong University of Science and Technology, Wuhan 430074, China (e-mail: lenc624@hust.edu.cn; zhangming_hust@126.com; kexunyu@163.com).

X. Q. Qin is with the School of Electrical Engineering and Automation, Hefei University of Technology, Hefei 230009, China (e-mail: 154227870@qq.com).

Z. Q. Song and P. Fu are with the Institute of Plasma Physics, Chinese Academy of Sciences, Hefei 230031, China (e-mail: zhquansong@ipp.ac.cn).

Color versions of one or more of the figures in this paper are available online at http://ieeexplore.ieee.org.

Digital Object Identifier 10.1109/TPS.2016.2585602

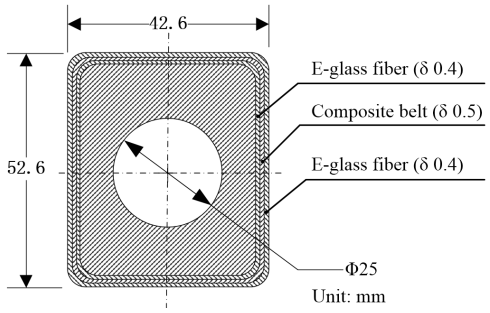

Fig. 2. Section view of aluminum coil with insulating materials.

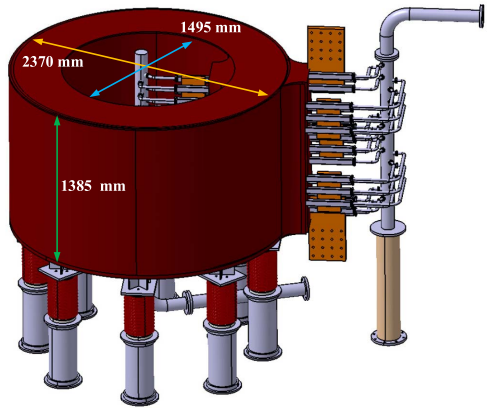

Fig. 3. 3-D dimensions and model of dummy load.

a structure of dry-type air-core water-cooling reactor with epoxy resin casting technique is presented. The pipe wire is a square cross-sectional hollow aluminum pipe with dimensions of 50 mm × 40 mm, a diameter 25 mm center hole for cooling water, and an edge radius of 3 mm. A full prototype is composed of eight parts connected in series. Each part has three nine-turn pipes connected in parallel with the identical average diameter of 1.924 m. Thus, the dummy load is 72 turns in total. Fig. 2 shows the section of aluminum coil with insulating materials, which mainly consist of E-glass fiber and composite belt [5]. The full 3-D dimensions and model are as shown in Fig. 3.

IV. FEM Analysis

As an essential component used to verify the capability of power supply systems, it is necessary to verify the thermal and dynamic stability, especially under the most extreme pulse operational mode. The finite-element analysis (FEA) has more accurate and visualized predictions compared with the traditional structure and heat theory, although FEA needs more detailed parameters about the model, material properties, boundary conditions, excitations, and so on [6]–[8]. This part shows the simulation results of the thermal and dynamic performance, especially under the extreme mode 68 kA lasting 15 s. In addition, the electromagnetic environment (EME) analysis and seismic analysis are also briefly introduced.

A. Structural Analysis

According to the various operational modes, the most extreme current is 68 kA. Therefore, it is necessary to verify

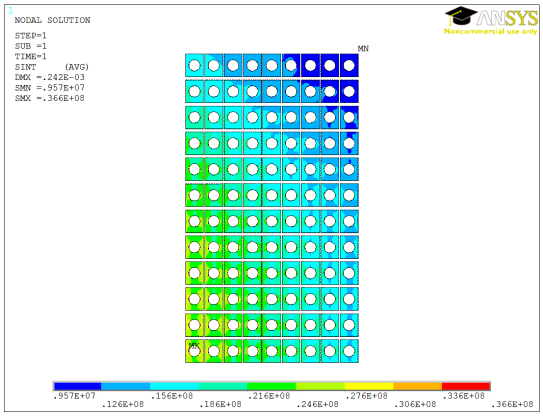

Fig. 4. Stress distribution of coil under 68 kA (Pa).

the mechanical performance of the whole structure, especially the aluminum coil. The 2-D model simulation is based on an FEM software. Due to the symmetry of the coil model, it is simplified to be 1/2 model to analyze the stress distribution. As shown in Fig. 4, the maximum stress of coil is about 36.6 MPa, which is less than the tensile strength 65.0 MPa for aluminum 6063-O from the supplier. The maximum stress position is located at the middle layer coils of the inner side of the prototype.

B. Thermal Analysis

Although the rated direct current is 7.75 kA, the pulse current can be up to 68 kA. Therefore, a visualized and accurate temperature variation of coil and water means a lot for the evaluation of the thermal performance and the design of the cooling water system. The prediction of the temperature variation is based on the combination of transient analysis and steady analysis. There are three typical operational stages, including steady stage, pulse stage, and off/zero-current stage. During the first stage, the thermal parameters can be calculated by the steady analysis [9]. As for the pulse stage, the results of the last step are transformed to the input data of the next step in the transient analysis, and iterate the calculation until it reaches the specified time. The accuracy can be assured by adjusting the convergence value and the step size. The transient analysis is also suitable for the third stage. During all the stages, the temperature of the inlet cooling water is 32 °C. For each pipe, the water velocity is 0.4 m/s, which means the total water flow is 17.0 m^3/h for dummy load. The water flows from the inside to the outside, through nine turns.

Fig. 5 shows the temperature distribution of a single aluminum pipe under the first steady stage 7.75 kA. As shown in Fig. 5, the maximum temperature of the coil is 42.2 °C during this stage.

Deduced from Fig. 6, the average temperature of the outlet water is 41.2 °C at this stage. The more detailed maximum temperature variation of coil and outlet water is described in Fig. 7. The temperature distribution at the steady stage (typical time a) has been described above. The temperature arises rapidly during the pulse stage. Then, it declines slowly due to the cooling water, as shown at the zero-current stage.

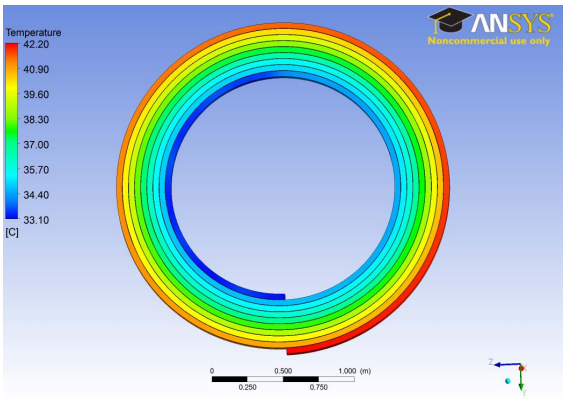

Fig. 5. Temperature distribution of coil at steady-stage 7.75 kA.

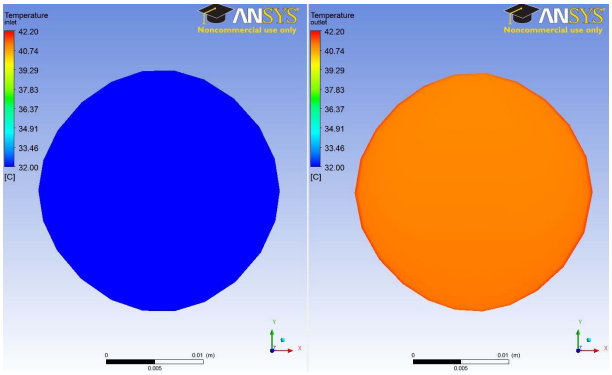

Fig. 6. Temperature distribution of inlet (left) and outlet (right) water at steady stage.

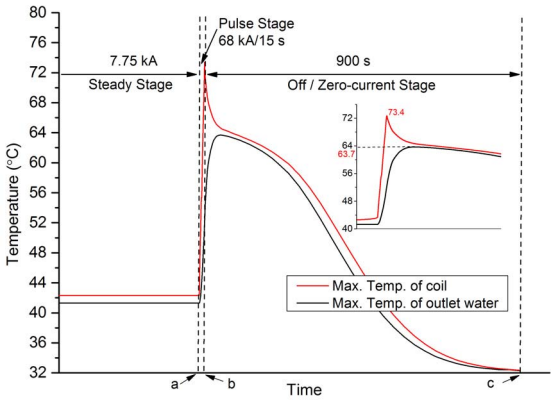

Fig. 7. Maximum temperature variation of coil and outlet water (a, b and c: three different moments).

The maximum temperatures of the coil and outlet water are 73.4 °C and 63.7 °C, respectively. At the end of one cycle, the temperature of the outlet water is approximately equal to that of the inlet water, which means the residual heat can be ignored. The detailed temperature distribution of coil at times b and c are shown in Fig. 8.

C. Electromagnetic Environment

Due to the large inductance and the pulse current, the magnetic field intensity around the dummy load should be taken into consideration, especially for the instrumentations selection and the delimitation of the personal safe area. Based on the combination of the Biot–Savart Law and the software MATLAB, the distribution is calculated by summing the magnetic flux intensity generated by each current element. The simplified 2-D size and model is shown in Fig. 9. From the data in Figs. 10 and 11, it can be seen that the radius of the safe area under steady stage and the most extreme pulse stage are 2.59 and 5.27 m, if the specified safe area means the magnetic flux intensity not exceeding 10 mT.

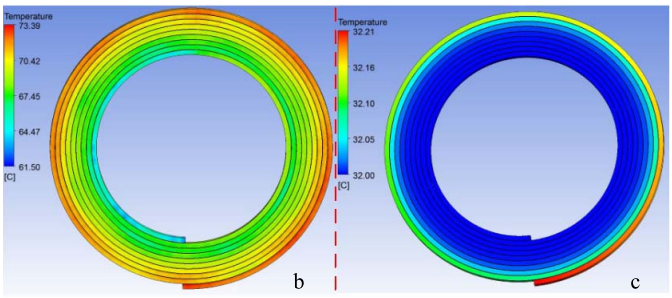

Fig. 8. Temperature distribution of coil at different moments. Distribution at moment b (left) and moment c (right), as shown in Fig. 7.

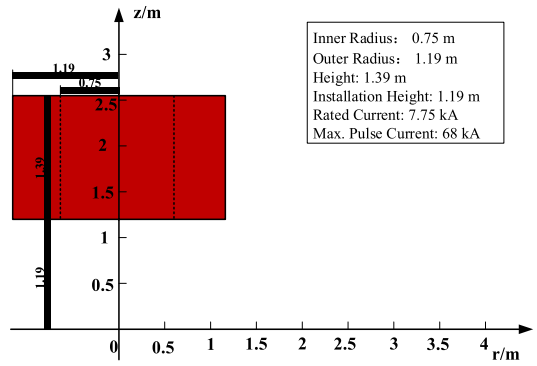

Fig. 9. Relative position and size of dummy load.

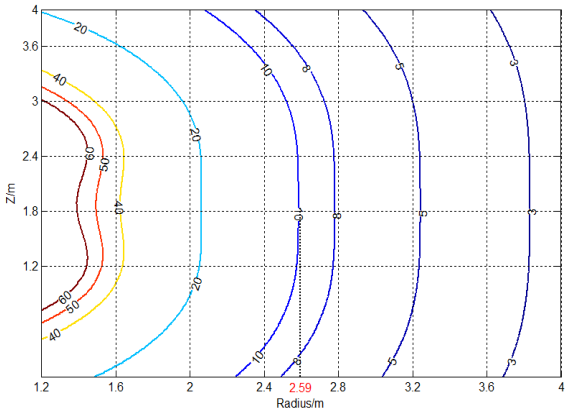

Fig. 10. Magnetic flux intensity (mT) distribution under 7.75 kA.

D. Seismic Analysis

According to the requirements of ITER, the equipment of the PF converter unit should restart without special mainte-

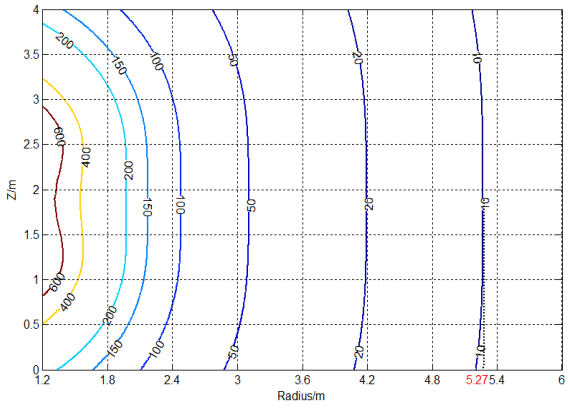

Fig. 11. Magnetic flux intensity (mT) distribution under 68 kA.

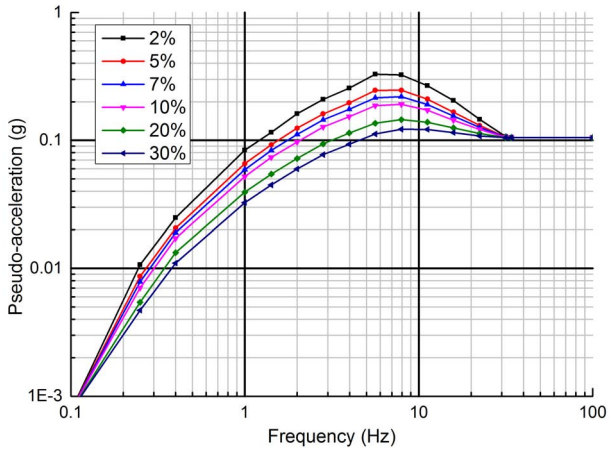

Fig. 12. Design earthquake spectrum of SL-1 with various damping factors in horizontal direction for ITER site Cadarache.

nance and test after the specific seismic events. Thus, it is essential to provide the seismic response information under specified seismic excitation. The analysis is based on the response spectrum method, which was first put forward in the 1940s by M Biot. The method is based on the assumption that the structure is a linear elastic multi-degree-of-freedom system. Thus, the linear elastic seismic response is decomposed into solving the largest earthquake response of each independent equivalent degree of freedom linear elastic system [10], [11]. The most extreme reaction force of support components exist in the combination of the results of each independent equivalent degree of freedom [12].

The design response spectrum for seismic level one (SL-1) with various damping factors for the site of Cadarache, provided by ITER, is as shown in Fig. 12. The damping factor 0.4 is adopted in the actual seismic analysis, and the value can be deduced from the curves using interpolation. In addition, values of pseudo-accelerations have to be multiplied by 2/3 in the vertical direction [13].

The basic analysis flow consists of static structural analysis, modal analysis, and response spectrum analysis combined with seismic excitation. Fig. 13 shows the deformation distribution in each direction under seismic excitation in the corresponding direction. The maximum deformation is about 4.1 mm.

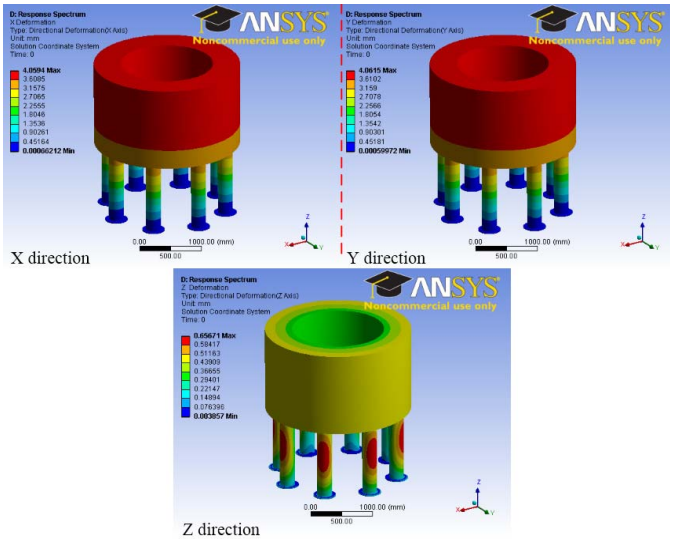

Fig. 13. Deformation distribution in each direction under seismic excitation in the corresponding direction.

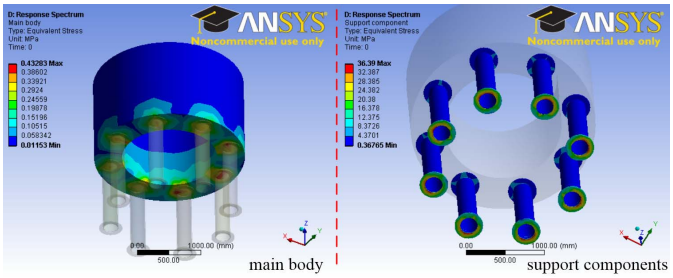

Fig. 14. Equivalent stress distribution under seismic excitation.

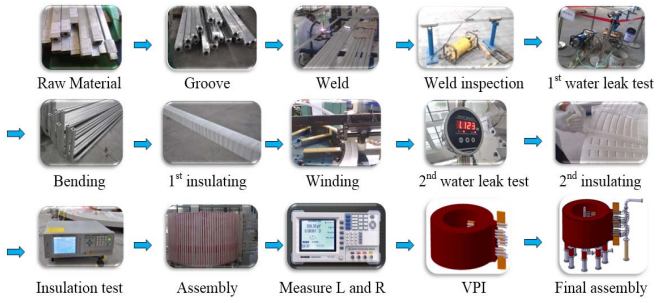

Fig. 15. Technological process of dummy load.

Fig. 14 describes the equivalent stress distribution under seismic excitation in the three directions. The maximum equivalent stress of the main body and support components are 0.44 and 36.39 MPa, respectively. Both of them are less than the allowable stress.

V. Fabrication Procedure

A visual presentation of the detailed fabrication procedures of dummy load is provided by the flowchart as shown in Fig. 15. The procedures are composed of four parts, including primary treatment, winding and inspection, vacuum pressure impregnation (VPI), and assembly. The first part

mainly includes raw material inspection, weld and inspection, and water leak test. The second part focuses on the procedures of single pipe, like the winding of coil, insulating treatment, turn-to-turn insulation test, and the measurement of inductance and resistance. The third part is VPI, which can improve the insulation level and reinforce the mechanical performance. The last part is the assembly of other accessories like support components, insulators, water pipes, and so on. Now, the process has come to the measurement of inductance and resistance. The next treatment is to cast the coils with VPI technique. After the assembly of the other accessories, tests specified by standard IEC 60076-6 will be carried out before the delivery.

VI. Conclusion

This paper mainly introduces the design of the dummy load prototype. Based on the FEM, the feasibility of the proposed structure has been evaluated, focusing on the thermal performance of the coil and the water-cooling system during the whole cycle and the dynamic stability, especially under the extreme pulse operational mode. The simulation results show the high feasibility and the feasibility of the proposed structure and design. In addition, the EME result shows that the radius of the safe area under 68 kA is 5.27 m, if the specified safe area means the magnetic flux intensity not exceeding 10 mT. The seismic analysis reflects the good antiseismic property of the dummy load under SL-1 with damping ratio 0.4. Lastly, the fabrication procedure is briefly introduced.

Acknowledgment

The authors would like to thank the Ministry of Science and Technology of China and the foundation and staff of ASIPP for helpful discussions and suggestions.

References

[1] P. Fu *et al.*, "Preliminary design of the poloidal field AC/DC converter system for the ITER coil power supply," *Fusion Sci. Technol.*, vol. 64, no. 4, pp. 741–747, 2013.

[2] P. L. Mondino, T. Bonicelli, V. Kuchinskiy, and A. Roshal, "ITER R&D: Auxiliary systems: Coil power supply components," *Fusion Eng. Des.*, vol. 55, no. 2, pp. 325–330, 2001.

[3] P. Fu *et al.*, "Review and analysis of the AC/DC converter of ITER coil power supply," in *Proc. IEEE Appl. Power Electron. Conf.*, Palm Springs, CA, USA, Feb. 2010, pp. 1810–1816.

[4] H. Yuan, P. Fu, G. Gao, and L. Huang, "On the circulating current control of ITER poloidal field converter," *J. Fusion Energy*, vol. 33, no. 3, pp. 269–274, 2014.

[5] C. Li, Z. Song, P. Fu, P. Wang, M. Zhang, and K. Yu, "Dynamic stability analysis of high-power DC reactor for ITER poloidal field converter," *J. Fusion Energy*, vol. 34, no. 2, pp. 202–206, 2015.

[6] R. Wrobel and P. H. Mellor, "Thermal design of high-energy-density wound components," *IEEE Trans. Ind. Electron.*, vol. 58, no. 9, pp. 4096–4104, Sep. 2011.

[7] D. A. Staton and A. Cavagnino, "Convection heat transfer and flow calculations suitable for electric machines thermal models," *IEEE Trans. Ind. Electron.*, vol. 55, no. 10, pp. 3509–3516, Oct. 2008.

[8] F. Marignetti, V. D. Colli, and Y. Coia, "Design of axial flux PM synchronous machines through 3-D coupled electromagnetic thermal and fluid-dynamical finite-element analysis," *IEEE Trans. Ind. Electron.*, vol. 55, no. 10, pp. 3591–3601, Oct. 2008.

[9] C. Li, Z. Song, P. Fu, M. Zhang, X. Zhang, and K. Yu, "Thermal design of high-power DC reactor for ITER poloidal field converter," *J. Fusion Energy*, vol. 33, no. 5, pp. 588–593, 2014.

[10] J. Sun, J.-J. Xu, and J. Weng, "Anti-seismic analysis of high voltage resistance box structure based on ANSYS workbench," *J. Mach. Design*, vol. 29, no. 2, pp. 72–75, 2012.

[11] Y. Liao *et al.*, "Seismic analysis of ITER poloidal field converter bridge," *J. Fusion Energy*, vol. 34, no. 1, pp. 70–75, 2015.

[12] G. Aiello *et al.*, "The ITER EC H and CD upper launcher: Seismic analysis," *Fusion Eng. Des.*, vol. 89, nos. 7–8, pp. 1809–1813, 2014.

[13] G. Sannazzaro, "Load specifications," ITER Org., Saint-Paul-lès-Durance, France, Tech. Rep. ITER IDM: 222QGL v6.0, Apr. 2012. [Online]. Available: https://user.iter.org/?uid=222QGL

Authors' photographs and biographies not available at the time of publication.